Relative Efficiencies for Parallel and Perpendicular Entrainment Flow Paths

T. P. Schmidt,* S. K. Ali,† and J. F. Foss‡
Michigan State University, East Lansing, Michigan

Abstract

HIGH-SPEED fluid, introduced into an otherwise quiescent region of ambient fluid, provides an effective means for inducing streamwise motion in the latter. Ejectors and jet-pumps are common technological examples of this phenomenon. The induced flow may be constrained to approach the high-speed flow with either a perpendicular or parallel orientation. The relative efficiency (as defined below) of these two entrainment flow paths is the primary subject of this paper.

The general problem under consideration is most readily described in terms of the specific investigation that was executed. The experimental geometry will be described and the relative efficiency will then be defined.

Figure 1 presents the parallel and perpendicular entrainment flow paths into the shear layer for the present experiment; these figures also allow a definition of the problem. Consider that a given high-speed or primary flow [viz., 50×80 cm, $U_0=13$ mps, $\theta(0)=9$ mm] exists and that a defined entrainment flow rate q_e will be delivered to the shear layer through a rectangular passage of width ℓ_e [viz., $\ell_e=150$ mm $=16.7\,\theta(0)$ and height $=80$ cm]. If the geometries of the entrainment plenums and the entrances to the entrainment channels are identical for the two entrainment paths, then the relative efficiency of the entrainment process can be characterized by the relative plenum pressure p_e to deliver the designated flow rate.

The present study also provides insight into the relationship between one- and two-stream layers. A two-stream mixing layer, in the limit as the low-speed velocity U_2 tends to zero, would be represented by the flow studied in Fig. 1a. This condition can be set in contrast to a single stream mixing layer (Fig. 1b) where the x-component velocity is identically zero as the fluid is introduced into the entrainment flow path. Since it is convenient to consider the limiting case: $U_2\rightarrow 0$ to be of the same "family" as $U_2=0$ (see, e.g., Brown and Roshko,[1] Fig. 10). It is useful to identify the similarities and differences of these two conditions.

Contents

The boundary conditions for the present experiment are established by 1) the primary flow boundary layer, 2) the streamwise variation of the inviscid flow conditions of the primary stream $U_0(x)$ or $p_0(x)$, and 3) the conditions within the entrainment plenum. Observations were not made in the entrainment plenum; the pressure was measured by an open tube at (2) in Figs. 1a and 1b, and it was assumed that negligible velocities (note the area ratio) existed in this region. The primary flow boundary layer (at separation) can be described by $\delta(x=0)=9$ cm and $R_\theta=7300$. Independent measurements of the velocity $U_0(x)$, and pressure $p_0(x)$, confirmed that there were no measurable accelerations in the primary flow over the region of interest $-2\le x/\ell\le 6$.

The entrainment flow rate was controlled by the use of a throttle plate and was metered by its passage through a slit-jet. Since the metering and throttling functions were independent, it was possible to create virtually the same entrainment flow for the two entrainment paths. That is, the precision and repeatability of this setting was better than its accuracy. The latter is estimated to be $V_e/U_0=0.05$, 0.04, 0.03 ± 0.0005 and was primarily limited by the ability to read the low ($\simeq$2-4 mps) velocities through the metering nozzle. Note that the selected entrainment velocities bracket, and stand well above, the nominal value for a single stream shear layer, $V_e/U_0=0.032$ (i.e., Liepmann and Laufer[2]).

The primary results are presented in Table 1. (The repeated data are second trials for the same conditions). The parallel case plenum pressures are approximately 38% larger than the perpendicular case pressures for the three V_e/U_0 values. This finding suggests that the entrainment processes for the parallel and perpendicular paths are rather different. The relatively large nondimensional values (based upon V_e) and their increase with decreasing (V_e/U_0) reveal a relatively large pressure drop coefficient associated with both cases. The relative constancy of the alternative nondimensional results—based upon the (V_e/U_0) product, is quite instructive. Apparently, this nondimensional form properly accounts for the combined effects of the plenum pressurization and the accelerative effects as the low-speed entrainment flow interacts with the high-speed primary flow.

The velocity surveys, in the entrainment channels for the two cases, clarify the reasons for the increased plenum pressure in the parallel case; see Fig. 2. Specifically, the mean velocity profile for the parallel case is highly skewed with a high-speed region near the splitter plate. In contrast, the perpendicular case exhibits a relatively flat velocity profile. Hence, for the same mass flux, the kinetic energy flux for the parallel case is substantially larger than that of the perpendicular case. The increased plenum pressure (p_e) must be present to account for this difference since the primary flow (i.e., the downstream pressure value for the entrainment flow) is identical in both cases. The kinetic energy

Table 1 Entrainment plenum pressure values

	$p_e^*=\frac{p_e-p_0}{(\frac{1}{2})\rho V_e^2}$		$p_e^{**}=\frac{p_e-p_0}{(\frac{1}{2})\rho V_e U_0}$	
V_e/U_0	Parallel	Perpendicular	Parallel	Perpendicular
0.05	10.84	7.78	0.542	0.389
0.05	10.93	7.92	0.547	0.396
0.04	13.97	10.21	0.559	0.408
0.04	13.89	10.29	0.556	0.412
0.03	19.83	14.25	0.595	0.428
0.03	19.87	14.26	0.596	0.428

Received May 13, 1985; synoptic submitted Dec. 20, 1985. Full paper available from National Technical Information Services, Springfield, VA 22157, at the standard price.

*Undergraduate Student, Department of Mechanical Engineering.
†Research Assistant, Department of Mechanical Engineering.
‡Professor, Department of Mechanical Engineering.

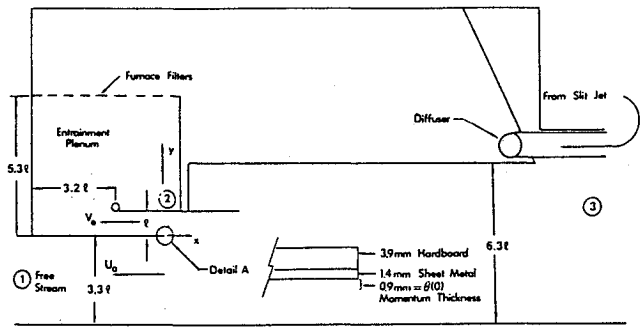

Fig. 1a Experimental configuration for the parallel entrainment flow path.

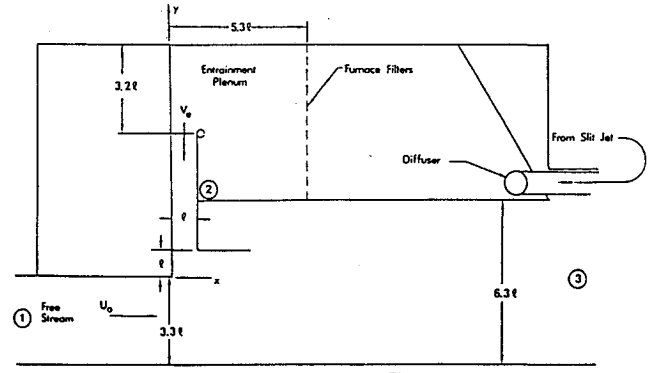

Fig. 1b Experimental configuration for the perpendicular flow path.

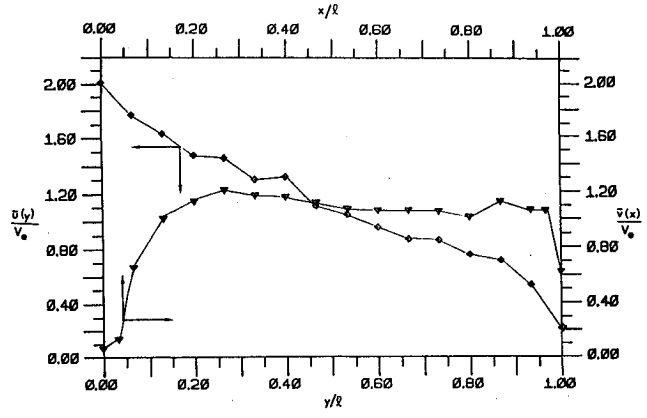

Fig. 2 Mean velocity distribution in the parallel entrainment channel [$\bar{u}(x=0,y)$] and in the perpendicular entrainment channel [$\bar{v}(x,y=15$ cm)].

flux correction factors (see, Potter and Foss[3]) provide a quantitative expression of this difference. The respective values, for the two cases, are α (parallel) = 2.02 and α (perpendicular) = 1.28. This percentage difference ($\simeq 58\%$) is even greater than that of the plenum pressures. The α values are defined as

$$\alpha \equiv \int V^2 V \cdot \hat{n} \mathrm{d}A / \langle V \rangle^3 A \tag{1}$$

and $\langle\ \rangle$ is used to designate a spatial average.

A downstream velocity survey $\bar{u}$ and $\tilde{u}$ at $x/\ell = 3$ [or $x/\theta(0) \simeq 5$] for the two cases, reveals that the developing shear layers are quite insensitive to the different entrainment paths, see Figs. 3a and 3b. (It is noted that a second downstream survey $x/\ell = 5$, that was not processed until the assembly was dismantled, showed differences in the mean velocity profiles. It is presumed that these differences, presented in the authors' full paper, reflect instrumentation

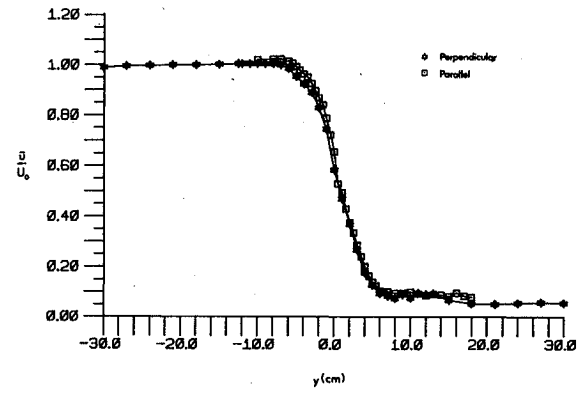

Fig. 3a Mean velocity surveys for the parallel and perpendicular cases at $x/\ell = 3$.

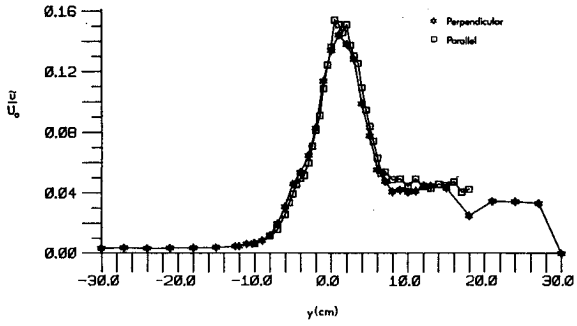

Fig. 3b Turbulence intensity profiles at $x/\ell = 3$.

problems and not an alteration of the turbulent stress field in the shear layer.) These experimental data allow the identification of the lateral position of the stream surface (y_s) which bounds the combined primary and entrainment stream flows.

$$q_s = q_p + q_e \text{ (per unit height)} \tag{2a}$$

$$q_s = U_0 \ell \int_{-0.8}^{0} \left(\frac{\tilde{u}}{U_0}\right)\Big]_{x=0} \frac{\mathrm{d}y}{\ell} + q_e \tag{2b}$$

$$q_s = U_0 \ell \int_{-0.8}^{y_s/\ell} \frac{\tilde{u}}{U_0}\Big]_x \frac{\mathrm{d}y}{\ell} \tag{2c}$$

Cubic splines were fit to the measured $\tilde{u}(y)$ data in order to evaluate the integrals for the two cases. The computed y_s/ℓ values were 2.4×10^{-2} (parallel) and 2.7×10^{-2} (perpendicular) at $x/\ell = 3$. (Similar values were obtained at $x/\ell = 5$.) A principle result from this computation is that a significant fraction of the low-speed streamwise flow at $x/\ell = 3$ is part of a recirculation pattern. Specifically, the mass flux associated with the positive velocity values between y_s and the outer wall of the test section, must be compensated by negative velocities (not measured) and a corresponding upstream mass flux since q_s represents the net flow rate through the test section. This result also helps to explain the insensitivity of the shear layer ($x/\ell = 3$) results to the strongly different initial conditions. Namely, the recirculatory flow is driven by relatively large turbulent stresses and it is reasonable to consider the recirculatory flow to be insensitive to the different initial conditions.

References

[1]Brown, G. L. and Roshko, A., "On Density Effects and Large Structure in Turbulent Mixing Layers," *Journal of Fluid Mechanics*, Vol. 64, 1974, pp. 775-816.

[2]Liepmann, H. W. and Laufer, J., "Investigation of Free Turbulent Mixing," NACA TN 1257, 1947.

[3]Potter, M. C. and Foss, J. F., *Fluid Mechanics*, Ronald Press Co., 1975.